

Detailed study of post-Chernobyl Cs-137 redistribution in the soils of a small agricultural catchment (Tula region, Russia)

Andrey P. Zhidkin^{a,*}, Evgeniya N. Shamshurina^b, Valentin N. Golosov^{b,c,d},
Mikhail A. Komissarov^e, Nadezhda N. Ivanova^b, Maxim M. Ivanov^{b,c}

^a V.V. Dokuchaev Soil Science Institute, Pyzhevskiy Pereulok 7, Moscow, 119017, Russian Federation

^b Faculty of Geography, Lomonosov Moscow State University, Leninskie Gory, GSP-1, Moscow, 119991, Russian Federation

^c Institute of Geography, Russian Academy of Sciences, Staromonetnyi Pereulok 29, Moscow, 119017, Russian Federation

^d Kazan (Volga Region) Federal University, Kremlevskaya Street, 18, Kazan, 420008, Russian Federation

^e Ufa Institute of Biology UFRS, Russian Academy of Sciences, Pr. Oktyabrya 69, Ufa, 450054, Russian Federation

ARTICLE INFO

Keywords:

Agricultural catchment
Chernobyl accident
East European plain
The Lokna river basin
Radioactive contamination
Radiocesium

ABSTRACT

A detailed study of ¹³⁷Cs redistribution was conducted within a small agricultural catchment in the highly contaminated Plavsk radioactive hotspot in the Tula region of Central Russia, 32 years after the Chernobyl nuclear power plant (NPP) accident, which occurred on April 26, 1986. Although more than three decades have passed since the Chernobyl NPP incident, ¹³⁷Cs contamination is high. The ¹³⁷Cs inventory varies from 67 to 306 kBq·m⁻², which is 2–6 times higher than the radiation safety standard; however, the soils remain suitable for crop cultivation. The initial ¹³⁷Cs fallout within the Plavsk radioactive hotspot was extremely heterogeneous, with a trend of decreasing ¹³⁷Cs inventories from the NW to the SE directions within the studied territory. Contemporary ¹³⁷Cs inventories are also very heterogeneous in the studied catchment. However, the trend of the initial ¹³⁷Cs fallout does not appear in the contemporary ¹³⁷Cs inventories on the slopes. Two methods of interpolation (expert-visual and automatic) were used to calculate the ¹³⁷Cs budget, revealing high similarity in their ¹³⁷Cs loss estimates; however, a large discrepancy was observed in their ¹³⁷Cs gain estimates. A detailed analysis of ¹³⁷Cs redistribution revealed the importance of hollows and “plow ramparts” (positive topographic forms on the boundaries of cultivated fields) in the transport and deposition of sediments. A quarter of the total ¹³⁷Cs gain was deposited within the arable land, whereas a quarter was deposited within the non-plowing sides of the dry valley; the other half was deposited in the valley bottom. About 7–8 × 10⁶ kBq of the ¹³⁷Cs inventory flowed out of the catchment area, which was only about 2% of the ¹³⁷Cs fallout after the Chernobyl NPP accident. About 89% of the total ¹³⁷Cs reserve is concentrated in the top (0–25 cm) layer of soils, regardless of land use or location within the catchment.

1. Introduction

The Chernobyl accident, which occurred on April 26, 1986, caused radioactive contamination across a large area of the East European Plain (EEP). More than 200 thousand km² of Europe was contaminated with radioactive ¹³⁷Cs (over 0.04 MBq of ¹³⁷Cs per m²), and 71% was deposited in the three most affected countries, Belarus, Russia, and Ukraine (Higley, 2006). Radio-Cs, or ¹³⁷Cs, is a relatively long-lived radionuclide with a half-life of 30.2 years. The spatial distribution of Chernobyl-derived ¹³⁷Cs fallout was controlled by two main factors: the trajectories of air mass transport and the intensity of precipitation 2–3

weeks after the explosion at the Chernobyl nuclear power plant (NPP) (Izrael et al., 1996; Gaydar and Nasvit, 2002). ¹³⁷Cs is rapidly and firmly adsorbed on mineral soil, particularly on fine and clay particles (Cho et al., 1996; Walling et al., 2006; Takahashi et al., 2017). The redistribution of ¹³⁷Cs within the EEP is associated with tillage erosion and the sheet, rill, and ephemeral gully erosion processes that occur during spring snowmelt (March–April) or summer rainstorms (Gusarov et al., 2019).

Some studies were conducted in the Plavsk radioactive hotspot area on the eastern track of the Chernobyl fallout (Golosov et al., 1999a, 2000, 2011; Kvasnikova et al., 2009; Ivanov et al., 2016; Mamikhin

* Corresponding author.

E-mail address: gidkin@mail.ru (A.P. Zhidkin).

<https://doi.org/10.1016/j.jenvrad.2020.106386>

Received 31 March 2020; Received in revised form 12 August 2020; Accepted 12 August 2020

Available online 7 September 2020

0265-931X/© 2020 Elsevier Ltd. All rights reserved.

et al., 2016; Komissarova and Paramonova, 2019). Golosov et al. (1999a, 2000) revealed considerable spatial heterogeneity in the center of the Plavsk radioactive hotspot: the inventories of ^{137}Cs varied from 368 ± 56 to $559 \pm 93 \text{ kBq}\cdot\text{m}^{-2}$ in arable chernozems located in different local interfluvies. A significant decrease in the ^{137}Cs content of arable soils on slopes, and the subsequent ^{137}Cs accumulation in the alluvial soils at the bottom of river valleys, were also recorded.

^{137}Cs budgets have been estimated during the study of global stratospheric depositions of radionuclides formed after nuclear bomb tests (Longmore et al., 1983; Vanden Berge and Gulinck, 1987; Sutherland and de Jong, 1990; Owens et al., 1997), and of tropospheric fallouts associated with accidents at NPPs (Walling et al., 2000; Panin et al., 2001; Golosov et al., 2018). Detailed estimates of the redistribution of sediments and ^{137}Cs were undertaken within small catchments (Ritchie et al., 1974; McHenry and Ritchie, 1975; Golosov et al., 1999b, 2013; Li et al., 2003; Ming-Yi et al., 2006; Porto et al., 2016; Varley et al., 2018). Studies conducted in the first decades after the Chernobyl accident did not indicate significant ^{137}Cs redistribution on eroded slopes (Litvin et al., 1996; Golosov and Markelov, 2002). However, ^{137}Cs reserves later increased in sediment sinks, particularly in dry valley bottoms, owing to the re-deposition of sediments, delivered by surface runoff from cultivated slopes (Fridman et al., 1997; Panin et al., 2001; Mamikhin et al., 2016).

^{137}Cs is one of the most dangerous pollutants; therefore, detailed studies of its migration are relevant and important. Like many other pollutants, ^{137}Cs reaches the soil surface with wet fallout and is rapidly and strongly adsorbed by clay and organic colloids within the soil (Ritchie et al., 1974). ^{137}Cs has limited mobility through chemical processes. Physical processes associated with the erosion, transport, and deposition of sediment particles, and with cultivation, represent the majority of ^{137}Cs redistribution (Sutherland and de Jong, 1990). The lateral migration trends obtained for ^{137}Cs can be used to predict the spatial redistribution of other pollutants that also appear from the atmosphere and are transported with solid matter (for example, polycyclic aromatic hydrocarbons, especially benzo[a]pyrene, heavy metals, hexachlorobenzene, DDT, other radionuclides, and many other pollutants). In previous publications (Samonova et al., 2015; Koshovskii et al., 2019) on the studied catchment, other pollutants (heavy metals and polycyclic aromatic hydrocarbons) and sediment transport were also analyzed. This study aimed to evaluate the spatial (lateral) and vertical redistribution features of Chernobyl-derived ^{137}Cs within a small agricultural catchment of the first order (Horton system), three decades after the Chernobyl incident.

2. Materials and methods

2.1. Study area

The study site is a small agricultural catchment located in the so-called “Plavsk Radioactive Spot” in the Tula region of Central Russia (Fig. 1A). This territory was recognized as one of the most radioactively contaminated areas in Russia after the Chernobyl accident, despite being located far from the Chernobyl NPP. An initial estimate of ^{137}Cs soil contamination in the “Plavsky Radioactive Spot” in 1986 was as high as $185\text{--}555 \text{ kBq}\cdot\text{m}^{-2}$ (Izrael and Bogdevich, 2009). Currently, the ^{137}Cs contamination remains extremely high (Evangelidou et al., 2016).

The catchment is in the northern part of the forest-steppe zone of the EEP and contains the right side tributary of the Lokna River (left tributary of the Plava River), 4 km south-west of Plavsk city (Fig. 1A). The catchment area is 0.96 km^2 (Fig. 1B). The studied catchment is used as tillage and is considered representative of the “Plavsky Radioactive Spot” territory in terms of relief, land use, and soil cover. Comparing the main morphometric characteristics of the studied catchment to other catchments of similar size in the Lokna River basin, allowed us to classify its main morphometric characteristics as typical (Table 1S).

The climate of the territory is moderately continental (*Dfb* according

to the Köppen-Geiger climate classification), with moderately cold winters and the warm summers. The coldest month is January (-9.7°C) and the warmest month is July ($+19.5^\circ\text{C}$). The average annual precipitation varies from 425–785 mm (<https://rp5.ru/>). The territory remains under snow for 115–130 days from December until March. The mean water reserve in the snow in March is 125–150 mm. The parent material is carbonate loess. Soil cover on the summit and upper parts of the slopes is represented by Luvic Greyzemec or Luvic Chernic Phaeozems (Loamic, Aric, and Pachic). On the lower parts of the slopes, the soil cover is dominated by Luvic Greyzemec Phaeozems (Epiloamic, Endoclayic, Aric, Differentic, and Episiltic). Soil erosion is observed mostly on cultivated slopes during spring snowmelt and heavy rainstorms (May–September).

The contemporary typical crop rotations include oats (*Avena*), wheat (*Triticum*), rye (*Secale cereale*), barley (*Hordeum*), buckwheat (*Fagopyrum esculentum*), potatoes (*Solanum tuberosum*), and soy (*Glycine max*). Earlier in the 1990s and 2000s, perennial grasses were included in the crop rotation. The non-plowed virgin parts of the catchment are occupied by grass communities including European slough-grass (*Beckmannia eruciformis*), meadow foxtail (*Alopecurus pratensis*), annual meadow grass (*Poa annua*), and tansies (*Tanacetum*).

The catchment has been used as tillage for more than 250 years (Atlas of Tula, 1784). The lower boundary of the plowed land is marked by “plow ramparts” (shafts), positive topographic forms 0.4–0.7 m high which appear at the edges of cultivated fields owing to the regular mechanical movement of soil during tillage. In the early 1990s, the boundary of the plowed land was moved further upslope and new plow ramparts were formed. Currently, two continuous plow ramparts of different ages can be easily identified along the lower boundary of the cultivated slopes (Fig. 1B).

2.2. Reference inventories of ^{137}Cs and reconstruction of the initial radioactive contamination

To check the initial Chernobyl-derived ^{137}Cs fallout, four reference plots were studied on relatively flat upper parts of the slopes (R1, R2, R3, and R4) at a distance 0.1–2.5 km from the studied catchment (Fig. 2). In reference plots R2, R3, and R4, bulk soil samples were collected using a hand sampler at 10 points arranged in a spiral (9 m wide) from depths of 0–25 and 25–50 cm. In reference plot R1, bulk soil samples were collected using a hand sampler at 20 points, arranged in two spirals.

The interpolation of the ^{137}Cs reference inventories was carried out in ArcGIS 10.1 using an inverse distance-weighted interpolation method. The initial ^{137}Cs fallout after the Chernobyl NPP accident was calculated by multiplying the interpolated reference inventories by the half-life coefficient of ^{137}Cs , which, for a period 32 years (1986–2018), is equal to 2.12.

2.3. Sampling and analytical measurements

Soil samples from the plowed land and abandoned plowed land were collected using a hand sampler (JMC, Newton, IA, USA; inner diameter: 4.5 cm) from depths of 0–25 and 25–50 cm at 77 sampling points along eight catenas (Fig. 1B). The selection of the sampling points in the sediment sink sites was based on an analysis of the terrain morphology. Within the uncultivated virgin parts of the catchment, incremental soil samples were collected, mainly from soil pits (1 m in length, 0.5 m in width, and 1.5 m deep). Five soil pits were excavated in the dry valley bottom (Fig. 3B, points T1, T3, T4, T5, T6) and five soil pits were studied on the sides of the valley (Fig. 3B, points B5, B6, B7, B8, B9). A detailed description of the soil profiles was conducted before sampling. The profile face with the lowest disturbance by bioturbation was selected for sampling. Soil samples were collected from a $15 \times 15 \text{ cm}$ area at 3–5 cm depth increments. In total, about 210 soil samples were collected using the hand sampler from 120 points (in the plowed and abandoned plowed land) and about 165 soil samples were collected from 10 soil pits (in the

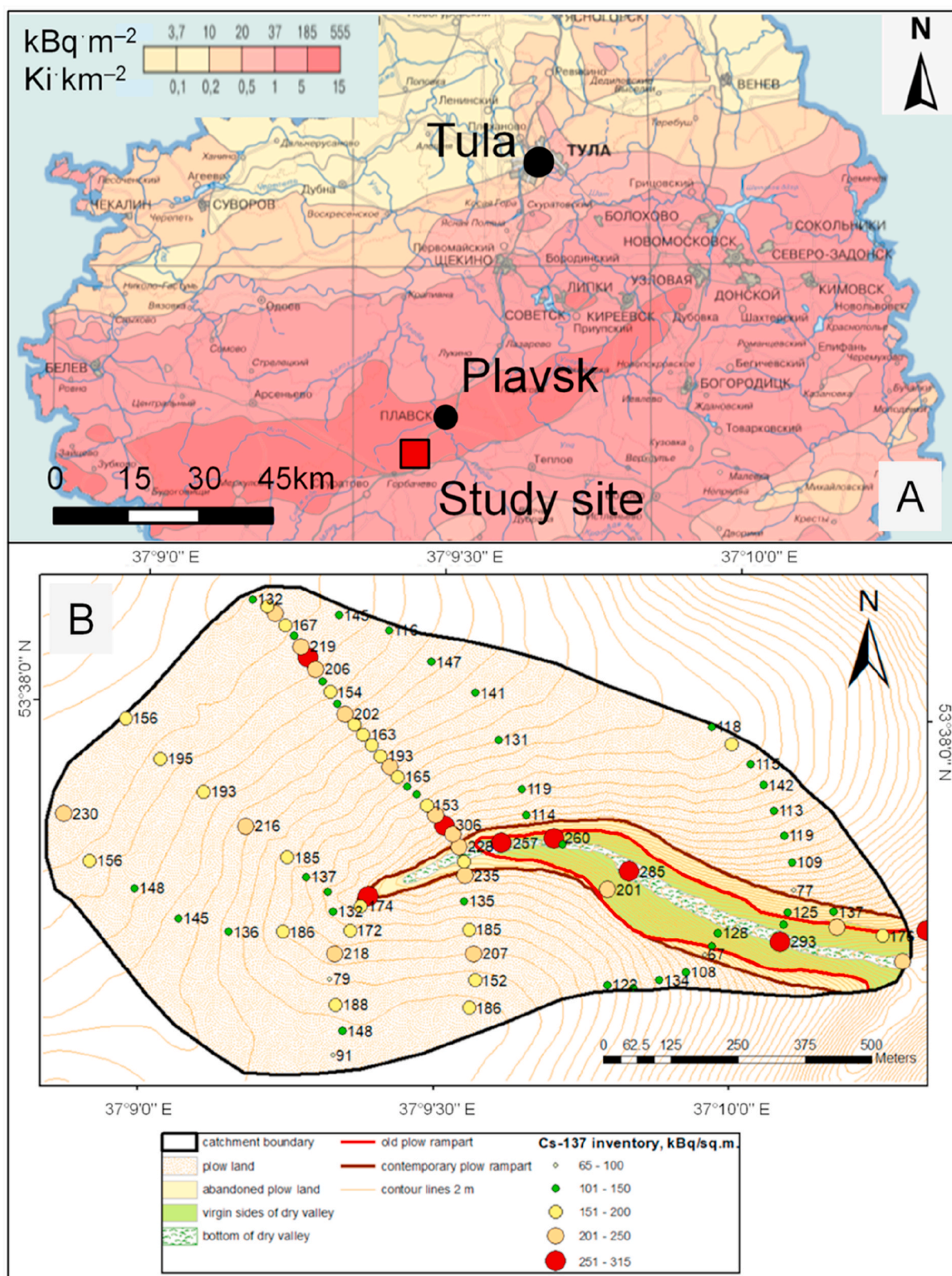


Fig. 1. ^{137}Cs contamination of the Tula region (Russia) after the Chernobyl nuclear power plant accident and the location of the study catchment (A); land use and topographic features of the studied catchment and contemporary ^{137}Cs inventories at the sampling points (B).

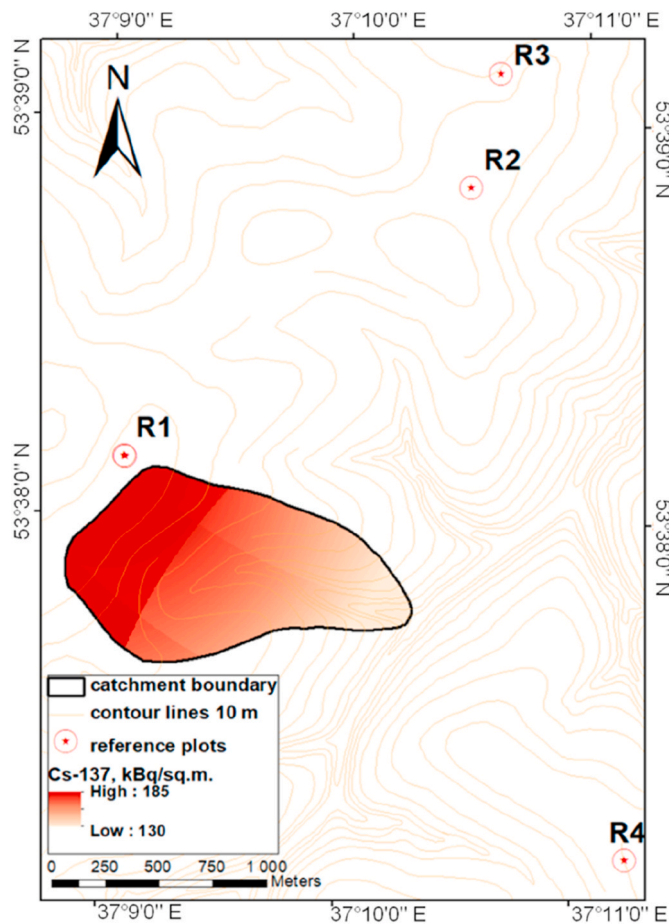


Fig. 2. Location of the reference plots and the interpolation of ^{137}Cs reference inventories within the studied catchment.

virgin part of the catchment).

The soil samples were oven-dried at 105 °C to constant weight, crushed using a mortar and pestle, sieved through 2-mm mesh, and prepared for γ -analysis. The ^{137}Cs activity of the homogenized samples was measured at 661.66 keV using a semiconductor gamma-ray spectrometer equipped with an HPGe detector. The spectrometers were manufactured by the Green Star Instruments company (type SKS-07 (09) P-G-R). With this equipment, the permissible fundamental relative error in measuring activity in point geometry is less than $\pm 10\%$. To unify the data obtained during several years of research, all ^{137}Cs inventories were recalculated taking the half-life of the radioisotope as of January 1, 2018 into account.

2.4. ^{137}Cs budget evaluation

2.4.1. Expert assessment

The catchment was divided into sections with different intensities of ^{137}Cs loss and gain (the plowed and non-plowed parts of the catchment separately). The individual sections of the slopes within the plowed land were allocated along the lines of local micro-watersheds, delineating the area according to morphological features (Fig. 3A). The morphometric characteristics of the selected sections were analyzed to confirm the validity of this visual separation. The following parameters were considered: slope steepness, longitudinal slope profile, and runoff line length (Tables 2S–4S). Currently, plowing is carried out on slopes with small gradients, rarely exceeding 6° (Table 2S). In general, slope gradient increases from the upper parts of the slope (section 5P) to its lower parts (sections 1P, 2P). Longitudinal slope profile changes from predominantly divergent in the upper sections of the catchment (section

5P) to divergent–convergent in the lower areas (sections 1P, 2P) (Table 3S). Runoff line length is distributed rather evenly across the different sections (Table 4S). However, section 4P is characterized by relatively high runoff line lengths. This can be explained by the presence of hollows, which cross the left side of the dry valley and act as pathway for temporary surface runoff. The catenas were considered representative for estimating ^{137}Cs redistribution within the sections. Each point participated equally in the estimation of the final average value of the change in radioisotope stocks.

On the sides and bottom of the dry valley, the redistribution of sediments is primarily controlled by the shapes of the slopes and their dissection by hollows. In addition to these natural factors, the redistribution of sediments is influenced by anthropogenic plow ramparts, which are artificial obstacles to downslope water flow and sediment transport. The non-plowed sides of the dry valley were divided into the following sections (Fig. 3B):

1S. The left and right sides of the dry valley in the middle and lower reaches. There are no hollows on the interfluvial slope. Two generations of continuous plow ramparts are clearly identifiable in the relief (Fig. 3B).

2S. The section in the headwater of the dry valley. The interfluvial slope and the side of a small valley on the left side are dissected by a series of subparallel hollows. The hollows cut through contemporary and old plow ramparts and stretch to the bottom of the dry valley, forming a fan imposed both on the bases of the sides and the bottom of the valley.

3S. The starboard area in the middle course. Only one plow rampart has formed in this section (the plowed land boundary has not been moved). One large hollow is clearly visible on the interfluvial slope above this section.

The dry valley bottom was divided into the following sections (Fig. 3B):

1B. The upper reaches of the dry valley bottom. It is now abandoned plowed land. This part of the bottom is a gentle hollow with no clearly defined sides. The contemporary plow ramparts are poorly identifiable in the relief. Numerous hollows stretch from the left side to the top of the dry valley.

2B. The middle reaches of the valley bottom, where it bends. The bottom width is only 4–5 m. The dry valley has a trapezoidal cross-section and the sides are well defined. Secondary cuts are detectable.

3B. The middle reaches of the valley bottom. A segment about 500 m long, fairly straight, and 25–40 m wide.

4B. The estuarine part of the valley bottom. The width is 12–15 m. The transverse profile of the valley is characterized by asymmetry, with a relatively flat left side and a steeper right side. There are secondary cuts.

The ^{137}Cs budget was calculated according to equation (1):

$$B = \sum_{i=1}^n [(\bar{x}_{Ci} - \bar{x}_{Ri}) \times Si] \quad (1)$$

where B is the total ^{137}Cs loss (negative value, $\text{kBq}\cdot\text{m}^{-2}$) or gain (positive value, $\text{kBq}\cdot\text{m}^{-2}$) within the catchment, \bar{x}_{Ci} is the arithmetic mean of the ^{137}Cs inventories ($\text{kBq}\cdot\text{m}^{-2}$) at all points inside section i, \bar{x}_{Ri} is the mean reference inventory ($\text{kBq}\cdot\text{m}^{-2}$) of the ^{137}Cs in section i, Si is the area of section i, and n is the number of sections.

2.4.2. Assessment by automatic GIS-interpolation

The automatic interpolation of the ^{137}Cs inventories was performed in ArcGIS 10.1 using the “Inverse Distance-Weighted Interpolation” method. Interpolation was carried out separately for the plowed and non-plowed parts of the catchment, and used all the sampling points

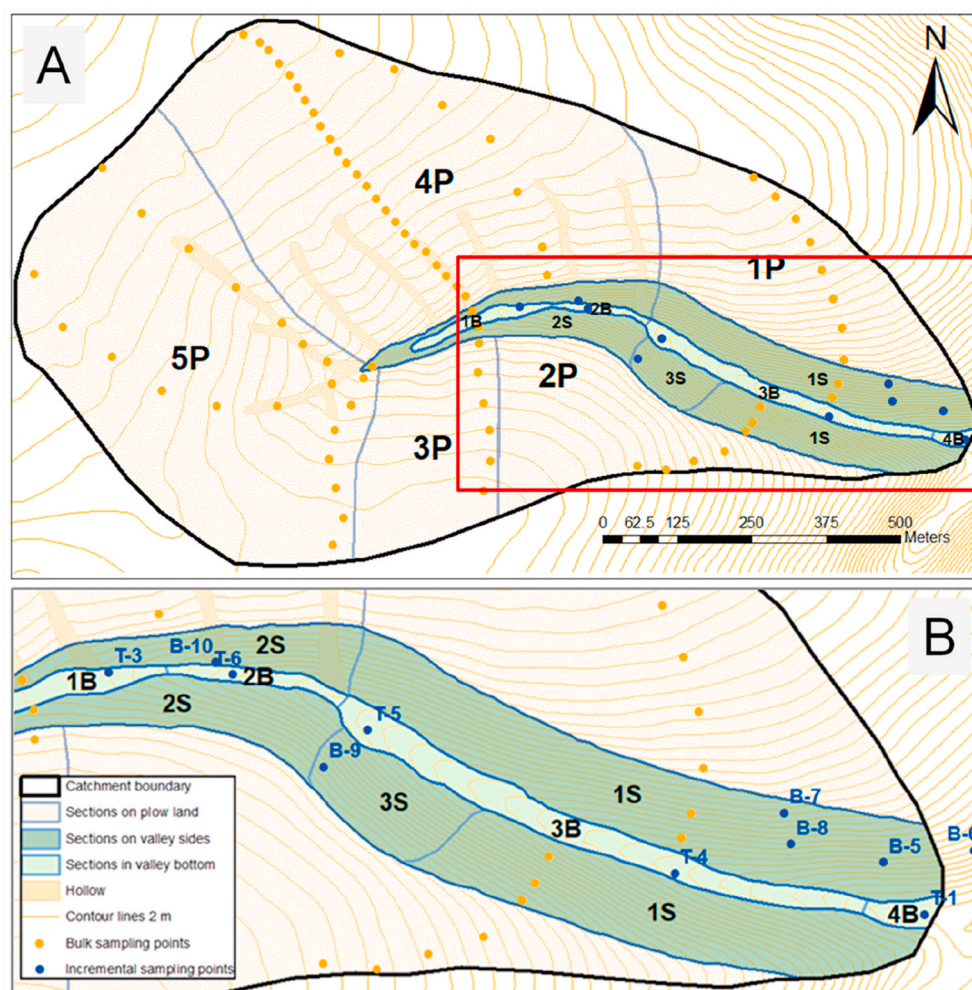


Fig. 3. General scheme of dividing of the whole catchment into sections and location of the sampling points (A) and scheme of dividing of the sides and the bottom of the dry valley into sections and location of the sampling points (B).

from the plowed or non-plowed land. The raster of the interpolated ^{137}Cs reference inventories was subtracted from the raster of the interpolated ^{137}Cs inventories for the sampling points using the “raster calculator” tool. The obtained rasters were exported in the form of tables. The sum of the negative values multiplied by the area of cells (4×4 m) constituted the loss component of the budget, while that of the positive values gave the gain component of the budget. The ^{137}Cs inventory removed through the catchment outlet was calculated as the difference between the ^{137}Cs losses and gains within the catchment.

3. Results

3.1. Reference inventory of ^{137}Cs and reconstruction of the initial ^{137}Cs contamination of the studied territory

There were significant differences in the average ^{137}Cs inventories across the reference plots. The maximum level was found in the R1 plot ($186 \pm 23 \text{ kBq}\cdot\text{m}^{-2}$), while the minimum was confined to the R4 plot ($73 \pm 6 \text{ kBq}\cdot\text{m}^{-2}$) (Fig. 2, Table 1). The average ^{137}Cs inventory in the reference plot soils was $135 \pm 24 \text{ kBq}\cdot\text{m}^{-2}$. Within plots R2 and R4, the coefficients of variation did not exceed 15% (Table 1), indicating sufficient homogeneity in the contamination density values within the sampling sites. In plot R1, the coefficient of variation of the ^{137}Cs inventories was 23%, and in plot R3, it was nearly the same (26%). Local variation in ^{137}Cs soil contamination was determined by the homogeneity of the radionuclide deposition from the atmosphere, the presence

Table 1

^{137}Cs inventory statistics for the reference plots (see Fig. 2 for their locations within the catchment).

Reference plots	Number of sampling points	Average ^{137}Cs inventory, $\text{kBq}\cdot\text{m}^{-2}$	Coefficient of variation of ^{137}Cs inventories, %
R1	20	186	23
R2	10	140	14
R3	10	141	26
R4	10	73	9

of rainfall after the accident, micro-landscape conditions at the sampling points (in particular, micro-relief features and pedoturbation), and local anthropogenic influences.

Fig. 2 shows the interpolation of ^{137}Cs reference inventories within the studied catchment. This map shows the presence of a gradient, with an increase in the ^{137}Cs initial fallout from $130 \text{ kBq}\cdot\text{m}^{-2}$ in the SE of the studied catchment to $185 \text{ kBq}\cdot\text{m}^{-2}$ in the NW. Thus, considering the period of decay, the initial fallout of ^{137}Cs after the Chernobyl NPP accident ranged from $276 \text{ kBq}\cdot\text{m}^{-2}$ in the SE of the studied catchment to $392 \text{ kBq}\cdot\text{m}^{-2}$ in the NW. These estimates, and the presence of a NW–SE gradient, correspond with the radiation pollution surveys carried out immediately after the Chernobyl NPP accident (Fig. 1A).

3.2. Contemporary distribution and budget of ^{137}Cs

Currently, there is strong variation in the soil ^{137}Cs inventories. The ^{137}Cs inventories at all the studied sampling points varied from 67 to 306 $\text{kBq}\cdot\text{m}^{-2}$ (Fig. 1B). Two-fold, and even almost three-fold, variations in ^{137}Cs inventories were recorded within 100–150 m slopes in the plowed land. Half of the investigated catenas revealed high ^{137}Cs inventories (207, 216, 218, and 219 $\text{kBq}\cdot\text{m}^{-2}$) in the central parts of the plowed slopes, exceeding the reference ^{137}Cs inventories by 20–30%. This likely indicates zones of intra-slope sediment accumulation in the plowed land.

The sides of the dry valley were divided into three sections. However, the research results revealed the necessity for a more detailed separation of these areas, which differed in their sediment redistribution processes. Sections 1S (Fig. 3B) was divided into the upper part, representing abandoned plowed land, and the lower part, which had never been plowed (virgin land). These parts are well distinguished by plow ramparts. In the upper part, the average ^{137}Cs inventory varied from 67 to 137 $\text{kBq}\cdot\text{m}^{-2}$ (110 $\text{kBq}\cdot\text{m}^{-2}$ on average) (Table 2), corresponding to ^{137}Cs loss. In the virgin part of the slope, the ^{137}Cs inventories varied from 128 to 228 $\text{kBq}\cdot\text{m}^{-2}$ (157 $\text{kBq}\cdot\text{m}^{-2}$ on average). Section 2S was also divided into two parts (inside and outside the hollows) characterized by different rates of sediment accumulation. The inventory of ^{137}Cs in the hollows was as high as 255–260 $\text{kBq}\cdot\text{m}^{-2}$, and the thickness of the sediment reached 12 cm (Table 2, Fig. 4, point B10). The vertical migration of ^{137}Cs in soil is very low and, without erosional processes and agricultural impacts (such as plowing, grassing, etc.), ^{137}Cs remains in the top layer (no deeper than 3 cm) for an extended period (Konoplev et al., 2016; Komissarov and Ogura, 2018). Thus, the ^{137}Cs peak in the deeper soil indicates accumulation of sediment above the peak. At point B10 (Table 2, Fig. 4), the peak of ^{137}Cs in the untilled hollows was found at a depth of 12 cm, owing to the burial of the initial peak layer by sediments delivered through surface runoff. The high inventory of ^{137}Cs indicates the accumulation of sediments washed away from the plowed land. The thickness of the post-Chernobyl period sediments were diagnosed using a diagram showing the vertical distribution of ^{137}Cs (Fig. 4). Outside the hollows the ^{137}Cs inventory was much lower (179 $\text{kBq}\cdot\text{m}^{-2}$), corresponding to low deposition. These results indicate that the hollows are important pathways of sediment and ^{137}Cs delivery to the bottom of the dry valley in this part of the catchment. All of section 3S is virgin land, and fairly homogeneous in terms of sediment deposition. The ^{137}Cs

reserve was 201 $\text{kBq}\cdot\text{m}^{-2}$ (Table 2). The thickness of the post-Chernobyl deposition layer was only 3 cm (point TPB-9, Fig. 4). In this section, the plowed land boundary remained unchanged over a considerably long period. The front part of the plow rampart is now practically filled with sediment. During extreme erosion events, the flow runs against the rampart and sediments are delivered to the virgin side of the dry valley.

Point B-6 is on the side of the valley in the lower reaches of the catchment, outside the natural catchment boundary (Fig. 3B). The ^{137}Cs reserve is extremely high at this point—313 $\text{kBq}\cdot\text{m}^{-2}$, which is the highest in all the studied territory. The thickness of the sediment deposited over the last 30 years was 12 cm. The sediment and ^{137}Cs accumulation at this spot are probably related to the influence of the plow rampart. In the lower reaches of the catchment, the plow rampart has a relative height of 1–1.5 m and a length of 200–300 m. Flowing water cannot overcome this rampart and runs along it until it turns. At the turn of the rampart, the front of it is filled with sediments, allowing the water to flow over the rampart and sediment to accumulate on the virgin side of the dry valley, outside the natural boundary of the catchment.

The bottom of the dry valley is the area of primary ^{137}Cs accumulation. Section 1B is in the upper part of the valley bottom (Fig. 3A and B). In this spot, the thickness of the post-Chernobyl sediment is about 8 cm, and the ^{137}Cs reserves are high (257 $\text{kBq}\cdot\text{m}^{-2}$) (Table 2). In section 2B (Fig. 3B), the width of the bottom is significantly narrower than in the adjacent sections. Numerous secondary incisions are visible in this part of the bottom. An almost two-fold decrease in ^{137}Cs reserves (119 $\text{kBq}\cdot\text{m}^{-2}$ at point T6) in the buried peak compared with the overlying layers, was recorded here. Thus, in this part of the bottom, sediment loss occurs simultaneously with sediment deposition. This is most likely caused by the concentration of the flow in the constriction, as well as the receipt of additional water and sediment from the left-bank hollow. Downstream of this, in section 3B, the bottom expands to 30–40 m (Fig. 3A), contributing to the formation of a deposition zone extending almost to the lower reaches of the dry valley. It contained extremely high ^{137}Cs reserves (285–293 $\text{kBq}\cdot\text{m}^{-2}$, points T4 and T5), as well as a thick layer (15 cm) of post-Chernobyl accumulation. In the lower reaches of the dry valley bottom (Fig. 3A and B, section 4B), secondary incisions appear again. The ^{137}Cs reserves decrease to 202 $\text{kBq}\cdot\text{m}^{-2}$ and the post-Chernobyl accumulation layer also decrease to 12 cm (Fig. 4, point T1). Thus, the mouth of the bottom is a transitional region, where both the transfer and deposition of solid material occur.

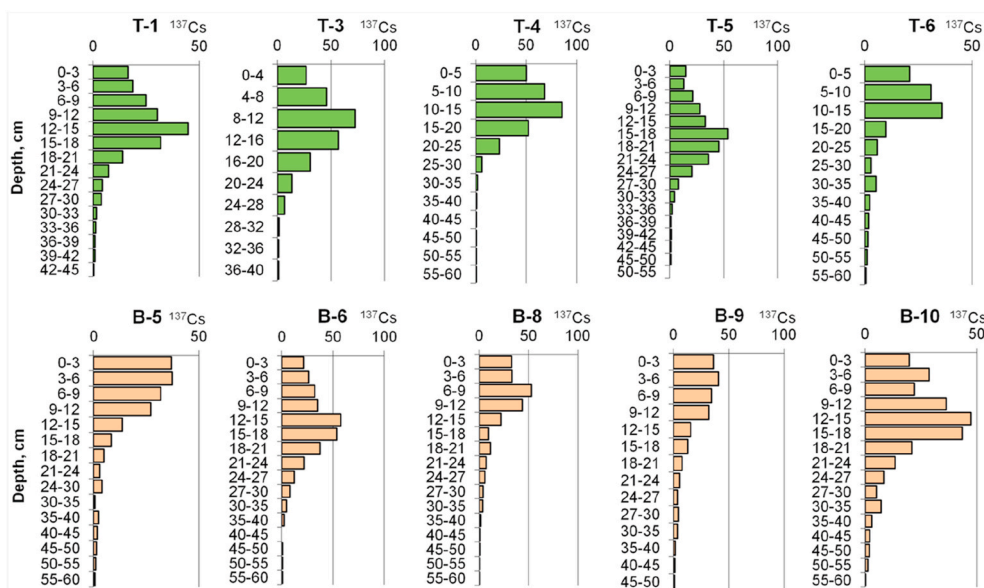


Fig. 4. The depth distribution of ^{137}Cs inventory ($\text{kBq}\cdot\text{m}^{-2}$) in the soils on the valley sides (top row; green color bars) and in the valley bottom (bottom row; brown color bars). (For interpretation of the references to color in this figure legend, the reader is referred to the Web version of this article.)

Table 3¹³⁷Cs budget estimated using different methods.

	Expert assessment ¹³⁷ Cs inventory, kBq × 10 ⁶	Automatic interpolation ¹³⁷ Cs inventory, kBq × 10 ⁶
Plowing part of the catchment		
Loss	12.7	14.0
Gain	1.1	2.7
Non-plowed parts of the catchment (sides and bottom of the dry valley)		
Loss	1.1	0.3
Gain	3.8	5.2
Entire catchment area		
Gross loss	13.8 (100%)	14.4 (100%)
Gain	4.9 (36%)	7.9 (55%)
Net loss	8.9 (64%)	6.5 (45%)

The ¹³⁷Cs budget is presented in Tables 2 and 3. In the plowed land, within sections 1P, 2P, 4P, and 5P, ¹³⁷Cs loss prevails, amounting to 12.7×10^6 kBq total ¹³⁷Cs loss from the plowed land. Within section 3P, the average ¹³⁷Cs inventory exceeded the initial ¹³⁷Cs contamination (taking radioactive decay into account), which may be owing to the deposition of sediments carried from upslope (from section 5P) or to calculation errors caused by the insufficiency of the spatial data on the initial ¹³⁷Cs contamination. The gain of ¹³⁷Cs in section 3P was 1.1×10^6 kBq (Table 3). On the sides and in the bottom of the dry valley, the total loss of ¹³⁷Cs was 1.1×10^6 kBq, and the gain was 3.8×10^6 kBq, according to the expert assessment. In particular, the ¹³⁷Cs gains on the sides of the dry valley were 1.5×10^6 kBq and the ¹³⁷Cs gain in the bottom of the dry valley was 2.3×10^6 kBq. Thus, about 25% of the total ¹³⁷Cs gain within the entire catchment was in the arable land area, about 25% on the sides of the dry valley, and about 50% in the valley bottom, according to the expert assessment.

The ¹³⁷Cs budget was also calculated using an alternative method of automatic interpolation. The estimates of ¹³⁷Cs loss obtained using the different methods were relatively similar, but the estimates of ¹³⁷Cs gain obtained using the different methods differed almost 2-fold (Table 3).

To identify the features of the vertical distribution of ¹³⁷Cs in soils, we compared the isotope reserves in the topsoil (upper 25 cm) with the total soil reserves (in 50 cm). At 20 points in the reference plots, the ¹³⁷Cs reserves in the upper 25-cm layer made up $87 \pm 8.8\%$ of those in the 50-cm layer. In the plowed land, this parameter amounted to $89 \pm 10.7\%$, using 66 points. In the virgin soils along the borders and bottom of the dry valley, this parameter amounted to $92 \pm 3.3\%$, using 10 points. The depth of the Chernobyl-derived ¹³⁷Cs peaks in the soil profiles at the sides and bottom of the dry valley did not exceed 15 cm. The average sediment accumulation depth was about 7 cm, corresponding to an average sediment accumulation rate of about 0.2 cm per year. In total, at the 96 sampling points, the ¹³⁷Cs reserves in the top 25-cm soil layer were $88.5 \pm 9.8\%$.

4. Discussion

The initial ¹³⁷Cs fallout within the Plavsk radioactive hotspot territory was very heterogeneous, as shown by the radiation pollution surveys carried out immediately after the Chernobyl NPP accident (Fig. 1A). The research revealed a clear SE–NW trend of ¹³⁷Cs reference inventories within the studied catchment. This trend is still clearly manifested at the sampling points in the flat upper parts of the slopes. However, this trend did not appear in the contemporary ¹³⁷Cs inventories of points in the plowed and eroded parts of the slopes, on the sides and at the bottom of the dry valley.

The heterogeneity of the initial ¹³⁷Cs fallout must be considered in the budget estimates. To reveal the effect of initial ¹³⁷Cs fallout heterogeneity, the ¹³⁷Cs budget was compared with one calculated based on the reference values taken from the nearest reference plot (R1) (Fig. 2). If the ¹³⁷Cs fallout heterogeneity is not taken into account, the calculations reveal a 1.8-fold increase in losses and a 2.5–4-fold decrease in

accumulation, depending on the method of interpolation used.

The ¹³⁷Cs budgets calculated using different methods are presented in Table 3. The differences in estimated ¹³⁷Cs losses are small—in the range of 0.6×10^6 kBq for the entire catchment. However, the differences in estimated ¹³⁷Cs gains are significant—in the range 3.0×10^6 kBq. The sides and bottom of the dry valley are characterized by high heterogeneity in their ¹³⁷Cs inventories. At a scale of tens of meters, a sharp change in ¹³⁷Cs reserves was recorded. For example, at point T4, the ¹³⁷Cs inventory was $293 \text{ kBq} \cdot \text{m}^{-2}$ and 30 m north (on the side of the dry valley) the ¹³⁷Cs inventory was only $128 \text{ kBq} \cdot \text{m}^{-2}$; and at point B10 on the side of the dry valley (in the hollow bottom) the ¹³⁷Cs inventory was $260 \text{ kBq} \cdot \text{m}^{-2}$ and 20 m away, at point T6 in the valley bottom, the ¹³⁷Cs inventory was only $119 \text{ kBq} \cdot \text{m}^{-2}$ (Figs. 1B and 2). Such high heterogeneity of ¹³⁷Cs inventories leads to the overstatement of ¹³⁷Cs gain when automatic interpolation is applied, while the expert-visual assessment should estimate the ¹³⁷Cs gain more accurately. However, the automatic interpolation method is more convenient for assessing changes in ¹³⁷Cs inventories on plowed slopes, especially when the heterogeneity of the initial ¹³⁷Cs fallout is taken into account. If sampling was carried out using a regular grid, rather than along the catenas, the differences in the sediment balances calculated by the different methods would probably be higher, and the automatic interpolation method would make it possible to estimate the ¹³⁷Cs budget in the plowed land more accurately. Thus, in our opinion, it is better to estimate ¹³⁷Cs budgets in plowed land using automatic interpolation, and on the sides and bottoms of the dry valley using expert assessment.

Budget calculations indicate that about of 35–55% of the ¹³⁷Cs that washed away from the plowed land was re-deposited inside the studied catchment on the sides and in the bottom of the dry valley, and in the bottoms of the hollows. The rest of the ¹³⁷Cs (45–65%) was washed out of the catchment (Table 3). These results do not contradict the data presented by Fridman et al. (1997) 10 years after the Chernobyl accident. The data showed that about 70% of the sediment entering the tributaries from the arable land was transported by flows to the bottom of the main valley. In general, the ¹³⁷Cs data for catchments of different sizes and regions differ significantly in the literature. Shamshurina (2009) studied a catchment (2 km²) located 300 km SW of Plavsk in Kursk Oblast. A significant portion of the slopes in this catchment (70%) underwent various anti-erosion measures. It was found that, from the total volume of ¹³⁷Cs displaced in solid runoff, about 80% was deposited within the slopes and at their base and 20% reached the bottom of the dry valley. The study of a small catchment area (14.8 km²) in southern Italy (Porto et al., 2014) showed that 63% of the ¹³⁷Cs reserves were significantly lower than the reference value, indicating the removal of the radionuclide, and about 22% were significantly higher, indicating accumulation. The authors concluded that, over the last decades, there had been a noticeable mobilization of Cs-containing sediments and 38% had moved out of the catchment area. In Spain (Navas et al., 2017), 28 fields with varying slope lengths, gradients, and time after land abandonment were selected for radioisotope studies. The local reference inventory was estimated at $4500 \text{ Bq} \cdot \text{m}^{-2}$. In the catchments, the average ¹³⁷Cs reserves in the upper parts of the slopes were $\sim 3900 \text{ Bq} \cdot \text{m}^{-2}$, while at the bottom of the slopes, where soil accumulation took place, it was higher ($\sim 5300 \text{ Bq} \cdot \text{m}^{-2}$). The deviations in ¹³⁷Cs reserve values from the reference plots were highest (over 20%) in the fields with the longest slopes. The greatest losses and gains of ¹³⁷Cs reserves were found in the fields with the longest duration of land abandonment, indicating a more intensive redistribution of soil particles. Irrespective of the timing of abandonment, the ¹³⁷Cs inventory ranges in the fields were found to be proportional to the water erosion index. Concurrently, Rodrigo-Comino et al. (2018) suggested that soil erosion rates depend on the duration of land abandonment; soil losses decrease with increasing abandonment duration.

In the plowed land the ¹³⁷Cs inventories vary from 77 to 306 $\text{kBq} \cdot \text{m}^{-2}$, on the sides of the dry valley the ¹³⁷Cs inventories vary from 67 to 313 $\text{kBq} \cdot \text{m}^{-2}$, and at the bottom of the dry valley the ¹³⁷Cs

Table 2
¹³⁷Cs inventories in the catchment sections (see Fig. 3 for their locations) and ¹³⁷Cs budget calculated by the expert assessment.

Section	Area of section, m ²	Number of sampling points	Reference ¹³⁷ Cs inventories average for the section, kBq m ⁻²	¹³⁷ Cs inventories (kBq m ⁻²) in points inside the section, min – max (mean)	¹³⁷ Cs loss (–)/gain (+), kBq × 10 ⁶	Share (%) of ¹³⁷ Cs loss (–)/gain (+) in section of total loss/gain in the catchment
1P	108000	8	152	77–151 (118)	–3.7	–27%
2P	83300	4	159	108–134 (125)	–2.8	–21%
3P	71400	6	167	135–235 (183)	1.1	23%
4P	297000	31	178	114–306 (174)	–1.3	–9%
5P	272000	21	181	79–230 (163)	–4.9	–35%
1S Abandoned plow land	28000	3	144	67–137 (110)	–1.0	–7%
1S Virgin land	40000	5	144	176–228 (157)	0.5	4%
2S Inside the hollows	4100	3	171	228–260 (248)	0.3	6%
2S Outside the hollows	24000	1	171	179	0.2	4%
3S	10100	1	157	201	0.4	9%
1B	4500	1	172	257	0.4	8%
2B	2000	1	170	119	–0.1	–1%
3B	12700	2	147	285–293 (289)	1.8	37%
4B	1500	1	132	202	0.1	2%
Total loss of ¹³⁷ Cs in the catchment					–13.8	–100%
Total gain of ¹³⁷ Cs in the catchment					4.9	100%

inventories vary from 119 to 293 kBq·m⁻². Thus, the ¹³⁷Cs inventories are very heterogeneous in the study catchment across all relief elements, regardless of land use.

The highest ¹³⁷Cs inventories were observed in the sediment accumulation zones, mainly confined to the lower parts of the studied catchment. Similar results, of higher ¹³⁷Cs inventories in lower slope sections, were found in other climatic conditions (Mabit et al., 2009; Navas et al., 2011; Komissarov and Ogura, 2017). However, a specific feature of the studied catchment is the large proportion of the intra-slope accumulation found in the arable land (about 25% of the total ¹³⁷Cs gain). Extremely high ¹³⁷Cs inventories were revealed in the hollow bottoms in the lower parts of the slopes and along the valley sides, indicating the significance of hollows in the migration of ¹³⁷Cs in sections 4P and 5P. In the bottom of the dry valley, about 50% of the total ¹³⁷Cs gain was detected. However, in some sections (2B, 4B), secondary incisions and relatively low ¹³⁷Cs inventories indicate simultaneous ¹³⁷Cs loss and gain. The intra-slope accumulation in the non-plowed sides of the dry valley in the estuary of the catchment was mainly associated with the presence of plow ramparts. They changed the direction of sediment flow, leading to the removal of part of the sediment in the main valley, bypassing the dry valley of the studied catchment. Therefore, the maximum ¹³⁷Cs inventories (313 kBq·m⁻²) were detected at point B-6 outside the natural boundary of the catchment, despite these sediments having been washed from plowed land in the catchment.

Analysis of ¹³⁷Cs depth distribution showed that the dominant ¹³⁷Cs reserves in the studied soils were in the top 25-cm layer: 87 ± 8.8% in the reference plots, 89 ± 10.7% in the plowed land, and 92 ± 3.3% in the virgin soils along the borders and bottom of the dry valley. The vertical migration of ¹³⁷Cs into the subsoil in the studied catchment is caused by diffusion, agro- and pedoturbations of the soil, and migration in dead roots holes and with live root secretions (Fokin et al., 2011). Many studies on the vertical distribution of radioactive Cs have indicated that most of the ¹³⁷Cs fallout remains in the soil surface layer (Arapis et al., 1997; Mamikhin et al., 2016), and in general, soil ¹³⁷Cs decreases steadily with increasing depth (e.g., Bunzl et al., 1995; Walling and He, 1999). Bunzl et al. (2002) established that most of the ¹³⁷Cs would accumulate in the root layer (0–7 cm) of a pasture, 20, 50, and 100 years after deposition. Komissarov and Ogura (2018) found that 80% of the total ¹³⁷Cs is accumulated at depths of 0–2.5 cm in untilled pastures, and 90% in the 0–20-cm layer in plowed fields. They also found that plowing reduces the air dose rate by 30–50%. Mabit et al. (2008) estimated that the ¹³⁷Cs activity in agricultural fields varied according depth. On average, around 65% of the total ¹³⁷Cs inventory was concentrated in the 0–20 cm depth increment, 25% in the 20–30 cm increment, and less than 10% in the last increment (30–40 cm) under the plow layer. In a cultivated field, where the upper soil layer is mixed annually by plowing, the ¹³⁷Cs is distributed uniformly and, with the exception of soils which adsorb this radionuclide only weakly, the deposited ¹³⁷Cs will essentially remain contained in this soil layer (Schimmack and Bunzl, 1986). In addition, plowing contaminated soil will dilute the radionuclides in a larger soil volume, and they will also have more contact with mineral surfaces, thus increasing their fixation to the frayed edge sites of clay minerals (Larsson, 2008).

The contemporary ¹³⁷Cs inventories in the soils of the studied catchment reached 306 kBq·m⁻². According to the radiological zoning of Russia (Russian Federal Law, 1991), the study area could therefore be classified into two zones: a) a zone with the right to resettlement—territory with a ¹³⁷Cs radionuclide soil contamination density of 185–555 kBq·m⁻² (5–15 Ki·km⁻²); and b) a residential zone with periodic radiation monitoring—a territory with a ¹³⁷Cs radionuclide soil pollution density of 37–185 kBq·m⁻² (1–5 Ki·km⁻²) in which the average annual effective dose to the population should not exceed 1 mSv per year (over the level of natural and technogenic background Cs). A territory with an average contamination density less than 37 kBq·m⁻² (1 Ki·km⁻²) is classified as free of radioactive contamination. Bruk et al. (2017) reported that the average annual effective dose (SGED₉₀) in the

Tula region in 2017 did not exceed 1 mSv per year. The SGED₉₀ was less than 0.3 mSv per year at 1195 settlements (out of a total of 1215 in the Tula region) and was between 0.3 and 1.0 mSv per year at only 20 settlements, with a maximum of 0.46 mSv per year.

The current ¹³⁷Cs reserves in soils used for agriculture in the studied catchment varied from 67 to 306 kBq·m⁻² in the plowed land and 67–293 kBq·m⁻² in the non-plowed land (virgin and abandoned plowed lands). According to regulatory documents (SanPiN, 2001; Join, 2004), the soil is suitable for agricultural production despite the high soil pollution levels. Land is considered fit for agricultural use if the reserves of ¹³⁷Cs and ⁹⁰Sr in the soil are below 1480 kBq·m⁻² (40 Ki·km⁻²) and 111 kBq·m⁻² (3 Ki·km⁻²), respectively (Russian Federal Law, 1991). The area of abandoned land in the Russian Federation where the soil radioactive contamination exceeds the permissible level and the lands are not considered suitable for agriculture, amount to 17.1 thousand ha (Jacob et al., 2009). Of this, 9.8 thousand ha is hayfields and pastures, and 7.3 thousand ha is plowed land. Approximately 2.9 million ha of agricultural land have been declared “radioactively contaminated,” with ¹³⁷Cs soil contamination densities above 37 kBq·m⁻² (Alexakhin et al., 2007). Therefore the Chernobyl accident had a strong effect on agricultural land use, which was a major segment of the national economy in the affected areas within the forest-steppe zone, where plowed soils, represented by fertile Chernozems and Phaeozems, exceeded 70% (Regions of Russia, 2016). In addition to soil contamination, land abandonment, and agricultural losses, the government does not receive taxes from these landowners as radioactively contaminated lands used in agriculture and forestry are often excluded from the land tax system. In this case, their cadastral value is only used as an element of the state cadaster of real estate for reference purposes (Makarov et al., 2016).

The catchment soils are suitable for crop production despite their high levels of ¹³⁷Cs contamination. This conclusion was derived from studies carried out in the same area by Komissarova and Paramonova (2019) and Schneider et al. (2008). Komissarova and Paramonova (2019) found that the density of ¹³⁷Cs soil contamination in the central part of the Plavsk radioactive hotspot ranged from 140 to 220 kBq·m⁻². In addition, the soil-to-plant transfer (TF) factor values are relatively small ($n \cdot 10^{-2}$ – $n \cdot 10^{-3}$), not exceeding and even less than those recommended by the IAEA's tentative ¹³⁷Cs TF values for agricultural crops growing in temperate climate conditions. Schneider et al. (2008) assessed the variability in ¹³⁷Cs accumulation in the vegetative parts of young and mature field-grown maize hybrid shoots and grains at different sites in the Tula region that were occupied by Luvic Chernozems with ¹³⁷Cs contamination levels of about 509–564 Bq kg⁻¹. It was found that the ¹³⁷Cs concentration ratios in the vegetative masses ranged from 1.07×10^{-2} to 2.79×10^{-2} in 2005 and from 1.60×10^{-2} to 3.30×10^{-2} in 2006. For grains, the values were between 0.26×10^{-2} and 0.61×10^{-2} in 2005 and between 0.38×10^{-2} and 0.79×10^{-2} in 2006. These values, being below 1.4×10^{-2} , can be characterized as permissible according to the classification recommended by Nisbet and Woodman (2000) for the mature edible parts of cereals grown on loamy soil.

5. Conclusion

¹³⁷Cs contamination in the center of the Plavsk radioactive hotspot is still high, with inventory levels 2–6 times higher than the safety standard. However, studies on ¹³⁷Cs plant uptake (Schneider et al., 2008; Komissarova and Paramonova, 2019) imply the possibility of growing crops in such conditions. The initial ¹³⁷Cs fallout was very heterogeneous, which must be taken into account in budget estimates. Total loss of ¹³⁷Cs from the catchment area over the last three decades was 6.5 – 8.9×10^6 kBq, which is only about 2% of the volume of the initial ¹³⁷Cs fallout. The redistribution of ¹³⁷Cs is largely controlled by hollows and plow ramparts. The hollows are important delivery pathways for sediment and ¹³⁷Cs to the bottom and the sides of the dry valley. The plow ramparts contribute to sediment and ¹³⁷Cs transport beyond the natural

boundary of the catchment. The valley bottom is the zone of predominant sediment and ¹³⁷Cs accumulation. However, locally, in the narrowing area and in the mouth of the bottom, both the deposition and loss of sediment and ¹³⁷Cs occur. A quarter of the ¹³⁷Cs total gain was deposited within the arable land, a quarter within the non-plowed sides of the dry valley, and half in the valley bottom. The intensity of translocation of ¹³⁷Cs into the subsurface horizons in Phaeozems is low. Over the past 30 years, only 11% of ¹³⁷Cs penetrated below the plowed horizon, the remaining 89% was preserved in the upper 25-cm layer. The peak of ¹³⁷Cs in the soil profiles on the sides and at the bottom of the dry valley did not exceed 15 cm. The results of this work illustrate the changes that have taken place in the radioactive hotspot after the Chernobyl NPP accident, and are also important for identifying the migration paths of various pollutants that might migrate with soil particles in an adsorbed form.

Declaration of competing interest

The authors declare that they have no known competing financial interests or personal relationships that could have appeared to influence the work reported in this paper.

Acknowledgements

This research was supported by the Russian Foundation for Basic Research (RFBR) within the scientific project N^o 18–35–20011.

Appendix A. Supplementary data

Supplementary data to this article can be found online at <https://doi.org/10.1016/j.jenvrad.2020.106386>.

References

- Alexakhin, R., Sanzhara, N., Fesenko, S., Spiridonov, S., Panov, A., 2007. Chernobyl radionuclide distribution, migration, and environmental and agricultural impacts. *Health Phys. Soc.* 93, 418–426. <https://doi.org/10.1097/01.HP.0000285093.63814.b7>.
- Arapis, G., Petrayev, E., Shagalova, E., Zhukova, O., Sokolik, G., Ivanova, T., 1997. Effective migration velocity of ¹³⁷Cs and ⁹⁰Sr as a function of the type of soils in Belarus. *J. Environ. Radioact.* 34, 171–185. [https://doi.org/10.1016/0265-931X\(96\)00013-6](https://doi.org/10.1016/0265-931X(96)00013-6).
- Atlas of Tula region ruled by governor general with statistical notes, Central state military historical archive of USSR (TsGVIA SSSR), MS 1784, No. 19121. (in Russian).
- Bruk, G.Y., Romanovich, I.K., Bazyukin, A.B., Bratilova, A.A., Vlasov, A.Y., Gromov, A.V., Zhesko, T.V., Kaduka, M.V., Kravtsova, O.S., Saprykin, K.A., Stepanov, V.S., Titov, N.V., Yakovlev, V.A., 2017. The average annual effective doses for the population of the settlements of the Russian Federation attributed to zones of radioactive contamination due to the Chernobyl accident (for the zonation purposes). *Radiation Hygiene* 10 (4), 73–78. <https://doi.org/10.21514/1998-426X-2017-10-4-73-78>.
- Bunzl, K., Kracke, W., Schimmack, W., Auerswald, K., 1995. Migration of fallout ²³⁹⁺²⁴⁰Pu, ²⁴¹Am and ¹³⁷Cs in the various horizons of a forest soil under pine. *J. Environ. Radioact.* 28, 17–34. [https://doi.org/10.1016/0265-931X\(94\)00066-6](https://doi.org/10.1016/0265-931X(94)00066-6).
- Bunzl, K., Schimmack, W., Zelles, L., Albers, B.P., 2002. Spatial variability of the vertical migration of fallout ¹³⁷Cs in the soil of a pasture, and consequences for long-term predictions. *Radiat. Environ. Biophys.* 39, 197–205. <https://doi.org/10.1007/s004110000062>.
- Cho, Y.H., Jeong, C.H., Hahn, P.S., 1996. Sorption characteristics of ¹³⁷Cs onto clay minerals: effect of mineral structure and ionic strength. *J. Radioanal. Nucl. Chem.* 204 (1), 33–43. <https://doi.org/10.1007/BF02060865>.
- Evangelou, N., Hamburger, T., Talerko, N., Zibitsev, S., Bondar, Y., Stohl, A., Balkanski, Y., Mousseau, T.A., Moller, A.P., 2016. Reconstructing the Chernobyl Nuclear Power Plant (CNPP) accident 30 years after. A unique database of air concentration and deposition measurements over Europe. *Environ. Pollut.* 216, 408–418. <https://doi.org/10.1016/j.envpol.2016.05.030>.
- Fokin, A.D., Lurie, A.A., Torshin, S.P., 2011. *Agricultural Radiology*, second ed. Lan', St. Petersburg (in Russian).
- Fridman, S.D., Kvasnikova, E.V., Glushko, O.V., Golosov, V.N., 1997. Migration of cesium-137 in associated complexes of the Central Russian Upland. *Russ. Meteorol. Hydrol.* 5, 45–55 (in Russian).
- Gaydar, A., Nasvit, O., 2002. Analysis of radioactive contamination in the near zone of Chernobyl NPP. In: *Recent Research Activities about the Chernobyl NPP Accident in Belarus, Ukraine and Russia*, vol. 79, pp. 59–73. KURRI-KR.

- Golosov, V.N., Belyaev, V.R., Markelov, M.V., 2013. Application of Chernobyl-derived ^{137}Cs fallout for sediment redistribution studies: lessons from European Russia. *Hydrol. Process.* 27 (6), 781–794. <https://doi.org/10.1002/hyp.9470>.
- Golosov, V.N., Gennadiev, A.N., Olson, K.R., Markelov, M.V., Zhidkin, A.P., Chendev, Yu.G., Kovach, R.G., 2011. Spatial and temporal features of soil erosion in the forest-steppe zone of the East-European Plain. *Eurasian Soil Sci.* 44 (7), 794–801. <https://doi.org/10.1134/S1064229311070064>.
- Golosov, V.N., Markelov, M.V., 2002. Application of Chernobyl-derived ^{137}Cs for assessment of soil redistribution in agricultural catchments of central Russia. In: Fernandez, Jean-Michel, Fichez, Renaud (Eds.), *Environmental Changes and Radioactive Tracer*. Centre IRD de Nouméa, pp. 367–383.
- Golosov, V.N., Panin, A.V., Markelov, M.V., 1999a. Chernobyl ^{137}Cs redistribution in the small basin of the Lokna river, Central Russia. *Phys. Chem. Earth* 24 (10), 881–885. [https://doi.org/10.1016/S1464-1895\(99\)00130-1](https://doi.org/10.1016/S1464-1895(99)00130-1).
- Golosov, V.N., Walling, D.E., Konoplev, A.V., Ivanov, M.M., Sharifullin, A.G., 2018. Application of bomb-and Chernobyl-derived radiocaesium for reconstructing changes in erosion rates and sediment fluxes from croplands in areas of European Russia with different levels of Chernobyl fallout. *J. Environ. Radioact.* 186, 78–89. <https://doi.org/10.1016/j.jenvrad.2017.06.022>.
- Golosov, V.N., Walling, D.E., Kvasnikova, E.V., Stukin, E.D., Nikolaev, A.N., Panin, A.V., 2000. Application of a field-portable scintillation detector for studying the distribution of ^{137}Cs inventories in a small basin in Central Russia. *J. Environ. Radioact.* 48, 79–94. [https://doi.org/10.1016/S0265-931X\(99\)00058-2](https://doi.org/10.1016/S0265-931X(99)00058-2).
- Golosov, V.N., Walling, D.E., Panin, A.V., Stukin, E.D., Kvasnikova, E.V., Ivanova, N.N., 1999b. The spatial variability of Chernobyl-derived ^{137}Cs inventories in small agricultural drainage basins in central Russia 11 years after the Chernobyl incident. *Appl. Radiat. Isot.* 51, 341–352. [https://doi.org/10.1016/S0969-8043\(99\)00050-0](https://doi.org/10.1016/S0969-8043(99)00050-0).
- Gusarov, A.V., Golosov, V.N., Ivanov, M.M., Sharifullin, A.G., 2019. Influence of relief characteristics and landscape connectivity on sediment redistribution in small agricultural catchments in the forest-steppe landscape zone of the Russian Plain within European Russia. *Geomorphology* 327, 230–247. <https://doi.org/10.1016/j.geomorph.2018.11.004>.
- Higley, K.A., 2006. *Environmental Consequences of the Chernobyl Accident and Their Remediation: Twenty Years of Experience*. International Atomic Energy Agency, Vienna, p. 166. ISBN.
- Ivanov, M.M., Ivanova, N.N., Golosov, V.N., Shamshurina, E.N., 2016. Assessing the accumulation of sorbed isotope ^{137}Cs within the upper components of the fluvial network in the zone of Chernobyl contamination. *Geogr. Nat. Resour.* 37 (4), 355–361. <https://doi.org/10.1134/S1875372816040107>.
- Izrael, Y.A., Bogdevich, I.M., 2009. Atlas of Modern and Forward-Looking Aspects of the Consequences of the Accident at the Chernobyl Nuclear Power Plant in the Affected Areas of Belarus and Russia. Belkartaographyia, Minsk–Moscow. Fund “Ionosphere” NIA-nature. (in Russian).
- Izrael, Y.A., De Cort, M., Jones, A.R., Nazarov, I.M., Fridman, S.D., Kvasnikova, E.V., Stukin, E.D., Kelly, G.N., Matveenko, I.I., Pokumeiko, Y.M., 1996. The Atlas of caesium-137 contamination of Europe after the Chernobyl accident. In: *Radiological Consequences of the Chernobyl Accident, Proceedings of the First International Conference*, pp. 1–10. EUR 16544 EN.
- Jacob, P., Fesenko, S., Bogdevitch, I., Kashparov, V., Sanzharova, N., Grebenshikova, N., Isamov, N., Lazarev, N., Panov, A., Ulanovsky, A., Zhuchenko, Y., Zhurba, M., 2009. Rural areas affected by the Chernobyl accident: radiation exposure and remediation strategies. *Sci. Total Environ.* 408, 14–25. <https://doi.org/10.1016/j.scitotenv.2009.09.006>.
- Minsk Join Manual for Agriculture in Radioactively Polluted Areas of Belarus and Russian Federation, 2004 (in Russian).
- Komissarov, M.A., Ogura, S., 2017. Distribution and migration of radiocaesium in sloping landscapes three years after the Fukushima-1 nuclear accident. *Eurasian Soil Sci.* 50 (7), 861–871. <https://doi.org/10.1134/S1064229317070043>.
- Komissarov, M.A., Ogura, S., 2018. The efficiency of moldboard plowing upon deactivation and rehabilitation of radioactively contaminated pastures in the North of Japan. *Eurasian Soil Sci.* 51 (8), 947–954. <https://doi.org/10.1134/S1064229318080057>.
- Komissarova, O., Paramonova, T., 2019. Land use in agricultural landscapes with chernozems contaminated after Chernobyl accident: can we be confident in radioecological safety of plant foodstuff? *International Soil and Water Conservation Research* 7 (2), 158–166. <https://doi.org/10.1016/j.iswcr.2019.03.001>.
- Konoplev, A.V., Golosov, V.N., Yoschenko, V.I., Nanba, K., Onda, Y., Takase, T., Wakiyama, Y., 2016. Vertical distribution of radiocaesium in soils of the area affected by the Fukushima Dai-ichi nuclear power plant accident. *Eurasian Soil Sci.* 49 (5), 570–580. <https://doi.org/10.1134/S1064229316050082>.
- Koshovskii, T.S., Zhidkin, A.P., Gennadiev, A.N., Ivanova, N.N., 2019. Diagnostics, genesis, and localization of pedosediments within a small catchment (central Russian upland). *Eurasian Soil Sci.* 52 (5), 481–493. <https://doi.org/10.1134/S1064229319050053>.
- Kvasnikova, E.V., Gordeev, S.K., Zhukova, O.M., Kirov, S.S., Konstantinov, S.V., Lysak, A.V., Manzon, D.A., 2009. Radioactive contamination of the central Russian upland and its surroundings 21 years after the Chernobyl NPP accident. *Russ. Meteorol. Hydrol.* 34 (11), 732–740. <https://doi.org/10.1068373909110053>.
- Larsson, M., 2008. *The Influence of Soil Properties on the Transfer of ^{137}Cs from Soil to Plant: Results from a Field Study 21 Years after the Chernobyl Accident* (Uppsala, Sweden).
- Li, Y., Poesen, J., Yang, J.C., Fu, B., Zhang, J.H., 2003. Evaluating gully erosion using ^{137}Cs and ^{210}Pb . *Soil Till. Res.* 69, 107–115. [https://doi.org/10.1016/S0167-1987\(02\)00132-0](https://doi.org/10.1016/S0167-1987(02)00132-0).
- Litvin, L.F., Golosov, V.N., Dobrovolskaya, N.G., Ivanova, N.N., Kiryukhina, Z.P., Krasnov, S.F., 1996. Redistribution of ^{137}Cs by the processes of water erosion of soil. *Water Resour.* 23 (3), 286–291.
- Longmore, M.E., O’Leary, B.M., Rose, C.W., Chandica, A.L., 1983. Mapping soil erosion and accumulation with the fallout isotope Caesium-137. *Aust. J. Soil Res.* 21 (4), 373–385. <https://doi.org/10.1071/SR9830373>.
- Mabit, L., Bernard, C., Makhlouf, M., Laverdiere, M.R., 2008. Spatial variability of erosion and soil organic matter content estimated from ^{137}Cs measurements and geostatistics. *Geoderma* 145, 245–251. <https://doi.org/10.1016/j.geoderma.2008.03.013>.
- Mabit, L., Klik, A., Benmansour, M., Toloza, A., Geisler, A., Gerstmann, U.C., 2009. Assessment of erosion and deposition rates within an Austrian agricultural watershed by combining ^{137}Cs , ^{210}Pb and conventional measurements. *Geoderma* 150, 231–239. <https://doi.org/10.1016/j.geoderma.2009.01.024>.
- Makarov, O.A., Tsvetnov, E.V., Shcheglov, A.I., Romashkina, A.D., Ermiyaev, Ya.R., 2016. Cadastral valuation of lands polluted with radionuclides. *Eurasian Soil Sci.* 49 (11), 1288–1293. <https://doi.org/10.1134/S1064229316110065>.
- Mamikhin, S.V., Golosov, V.N., Paramonova, T.A., Shamshurina, E.N., Ivanov, M.M., 2016. Vertical distribution of ^{137}Cs in alluvial soils of the Lokna river floodplain (Tula oblast) long after the Chernobyl accident and its simulation. *Eurasian Soil Sci.* 49 (12), 1432–1442. <https://doi.org/10.1134/S1064229316120103>.
- McHenry, J.R., Ritchie, J.C., 1975. Redistribution of caesium-137 in southeastern watersheds. In: *Mineral Cycling in Southeastern Ecosystems*, 452–461. Energy Research and Development Administration (ERDA), Washington, DC, USA, pp. 74–740513. Symposium series. CONF.
- Ming-Yi, Y., Jun-Liang, T., Pu-Ling, L., 2006. Investigating the spatial distribution of soil erosion and deposition in a small catchment on the Loess Plateau of China, using ^{137}Cs . *Soil Till. Res.* 87 (2), 186–193. <https://doi.org/10.1016/j.still.2005.03.010>.
- Navas, A., Gaspar, L., Quijano, L., López-Vicente, M., Machin, J., 2011. Patterns of soil organic carbon and nitrogen in relation to soil movement under different land uses in mountain fields (South Central Pyrenees). *Catena* 94, 43–52. <https://doi.org/10.1016/j.catena.2011.05.012>.
- Navas, A., Quine, T.A., Walling, D.E., Gaspar, L., Quijano, L., Lizaga, I., 2017. Relating intensity of soil redistribution to land use changes in abandoned Pyrenean fields using fallout caesium-137. *Land Degrad. Dev.* <https://doi.org/10.1002/ldr.2724>.
- Nisbet, A.F., Woodman, R.F.M., 2000. Soil-to-plant transfer factor for radiocaesium and radiostrontium in agricultural systems. *Health Phys.* 78 (3), 279–288. <https://doi.org/10.1097/00004032-200003000-00005>, 2000.
- Owens, P.N., Walling, D.E., He, Q., Shanahan, J., Foster, I.D.L., 1997. The use of caesium-137 measurements to establish a sediment budget for the Start catchment, Devon, UK. *Hydrol. Sci. J.* 42 (3), 405–423. <https://doi.org/10.1080/02626669709492037>.
- Panin, A.V., Walling, D.E., Golosov, V.N., 2001. The role of soil erosion and fluvial processes in the post-fallout redistribution of Chernobyl-derived caesium-137: a case study of the Lapki catchment, Central Russia. *Geomorphology* 40, 185–204. [https://doi.org/10.1016/S0169-555X\(01\)00043-5](https://doi.org/10.1016/S0169-555X(01)00043-5).
- Porto, P., Walling, D.E., Alewell, C., Callegari, G., Mabit, L., Mallimo, N., Meusburger, K., Zehring, M., 2014. Use of a Cs-137 re-sampling technique to investigate temporal changes in soil erosion and sediment mobilisation for a small forested catchment in southern Italy. *J. Environ. Radioact.* 138, 137–148. <https://doi.org/10.1016/j.jenvrad.2014.08.007>.
- Porto, P., Walling, D.E., La Sparda, C., Callegari, G., 2016. Validating the use of ^{137}Cs measurements to derive the slope component of the sediment budget of a small rangeland catchment in southern Italy. *Land Degrad. Dev.* 27, 798–810. <https://doi.org/10.1002/ldr.2388>.
- Regions of Russia, 2016. *Socio-economic Indicators. Statistical Compilation*. Rosstat, Moscow, Russia (in Russian).
- Ritchie, J.C., McHenry, J.R., Gill, A.C., 1974. Fallout ^{137}Cs in the soils and sediments of three small watersheds. *Ecol.* 55, 887–890. <https://doi.org/10.2307/1934426>.
- Rodrigo-Comino, J., Martínez-Hernández, C., Iserloh, T., Cerda, A., 2018. Contrasted impact of land abandonment on soil erosion in Mediterranean agriculture fields. *Pedosphere* 28 (4), 617–631. [https://doi.org/10.1016/S1002-0160\(17\)60441-7](https://doi.org/10.1016/S1002-0160(17)60441-7).
- Russian Federal Law No 1244-1 of May 15, 1991. On social support of people subjected to radiation during the Chernobyl disaster. updated on December 28, 2016. http://www.consultant.ru/document/cons_doc_LAW_5323.
- Samonova, O.A., Gennadiev, A.N., Koshovskii, T.S., Zhidkin, A.P., 2015. Metals in the soils of a small watershed in the forest-steppe zone of the central Russian upland. *Eurasian Soil Sci.* 48 (6), 584–592. <https://doi.org/10.1134/S1064229315060101>.
- SanPiN 2.3.2.1078-01, SanPiN 2.3.2.2650-10, 2001. *Hygienic Requirements to the Safety and Nutritive Value of Food*. Moscow. (in Russian).
- Schimmack, W., Bunzl, K., 1986. Migration of radionuclides in a cultivated soil: effect of ploughing. *Geoderma* 81 (3–4), 313–337. [https://doi.org/10.1016/0016-7061\(86\)90012-1](https://doi.org/10.1016/0016-7061(86)90012-1).
- Schneider, K., Kuznetsov, V.K., Sanzharova, N.I., Kanter, U., Telikh, K., Khlopuk, M., 2008. Soil-to-plant and soil-to-grain transfer of ^{137}Cs in field-grown maize hybrids during two contrasting seasons: assessing the phenotypic variability and its genetic component. *Radiat. Environ. Biophys.* 47, 241–252. <https://doi.org/10.1007/s00411-008-0158-z>.
- Shamshurina, E.N., 2009. Radioecological aspects of recent soil contamination in small catchments of Kursk oblast. *Moscow Univ. Soil Sci. Bull.* 64, 26–32. <https://doi.org/10.3103/S0147687409010050>.
- Sutherland, R.A., de Jong, E., 1990. Estimation of sediment redistribution within agricultural fields using caesium-137. *Crystal Springs, Saskatchewan, Canada. Appl. Geogr.* 10 (3), 205–221. [https://doi.org/10.1016/0143-6228\(90\)90022-H](https://doi.org/10.1016/0143-6228(90)90022-H).
- Takahashi, S., Suchara, I., Okamoto, K., Sucharova, J., Umegaki, K., Fujiyoshi, R., 2017. Retention of ^{137}Cs in forest floor at three temperate coniferous forest stands in the Czech Republic diversely affected by fallout after the Chernobyl disaster in 1986.

- J. Radioanal. Nucl. Chem. 311, 929–935. <https://doi.org/10.1007/s10967-016-5048-2>.
- Vanden Berghe, I., Gulinck, H., 1987. Fallout ^{137}Cs as a tracer for soil mobility in the landscape framework of the Belgian loamy region. *Pedologie* 37, 5–20.
- Varley, A., Tyler, A., Bondar, Y., Hosseini, A., Zabrotski, V., Dowdall, M., 2018. Reconstructing the deposition environment and long-term fate of Chernobyl ^{137}Cs at the floodplain scale through mobile gamma spectrometry. *Environ. Pollut.* 240, 191–199. <https://doi.org/10.1016/j.envpol.2018.04.112>.
- Walling, D.E., Collins, A.L., Jones, P.A., Leeks, G.J.L., Old, G., 2006. Establishing fine-grained sediment budgets for the Pang and Lambourn LOCAR catchments, UK. *J. Hydrol.* 330, 126–141. <https://doi.org/10.1016/j.jhydrol.2006.04.015>.
- Walling, D.E., Golosov, V.N., Panin, A.V., He, Q., 2000. Use of radiocaesium to investigate erosion and sedimentation in areas with high levels of Chernobyl fallout. In: *Tracers in Geomorphology*. John Wiley & Sons, pp. 183–200.
- Walling, D.E., He, Q., 1999. Improved models for estimating soil erosion rates from Caesium-137 measurements. *J. Environ. Qual.* 28, 611–622. <https://doi.org/10.2134/jeq1999.00472425002800020027x>.